Photobioreactor design for isotopic non-stationary 13 C-metabolic flux analysis (INST 13 C-MFA) under photoautotrophic conditions

Arnaud Martzolff, Stephane Massou, Edern Cahoreau, Guillaume Cogne, Lindsay Peyriga, Jean-Charles Portais, Emmanuel Dechandol, Fabienne Le Grand, Stéphane Massou, Olivier Gonçalves, et al.

Photobioreactor Design for Isotopic Non-Stationary ^{13}C-Metabolic Flux Analysis (INST ^{13}C-MFA) Under Photoautotrophic Conditions

Arnaud Martzolff,[1] Edern Cahoreau,[2,3,4] Guillaume Cogne,[1] Lindsay Peyriga,[2,3,4] Jean-Charles Portais,[2,3,4] Emmanuel Dechandol,[1] Fabienne Le Grand,[1] Stéphane Massou,[2,3,4] Olivier Gonçalves,[1] Jérémy Pruvost,[1] Jack Legrand[1]

[1]LUNAM Université, Université de Nantes, CNRS, GEPEA, UMR 6144, Bât. CRTT, 37 boulevard de l'Université, BP 406, F-44602 Saint-Nazaire Cedex, France; telephone: +33-2-40-17-26-11; fax: +33-2-40-17-26-18; e-mail: guillaume.cogne@univ-nantes.fr

[2]Université de Toulouse, INSA, UPS, INP, Toulouse, France

[3]INRA, UMR 792, Ingénierie des Systèmes Biologiques et des Procédés, Toulouse, France

[4]CNRS, Toulouse, France

ABSTRACT: Adaptive metabolic behavior of photoautotrophic microorganisms toward genetic and environmental perturbations can be interpreted in a quantitative depiction of carbon flow through a biochemical reaction network using isotopic non-stationary ^{13}C-metabolic flux analysis (INST ^{13}C-MFA). To evaluate ^{13}C-metabolic flux maps for *Chlamydomonas reinhardtii*, an original experimental framework was designed allowing rapid, reliable collection of high-quality isotopomer data against time. It involved (i) a short-time ^{13}C labeling injection device based on mixing control in a torus-shaped photobioreactor with plug-flow hydrodynamics allowing a sudden step-change in the ^{13}C proportion in the substrate feed and (ii) a rapid sampling procedure using an automatic fast filtration method coupled to a manual rapid liquid nitrogen quenching step. ^{13}C-substrate labeling enrichment was controlled through the total dissolved inorganic carbon concentration in the pulsed solution. First results were obtained from steady-state continuous culture measurements allowing the characterization of the kinetics of label incorporation into light-limited growing cells cultivated in a photobioreactor operating at the maximal biomass productivity for an incident photon flux density of 200 μmol m^{-2} s^{-1}. ^{13}C label incorporation was measured for 21 intracellular metabolites using IC-MS/MS in 58 samples collected across a labeling experiment duration of 7 min. The fastest labeling rate was observed for 2/3-phosphoglycerate with an apparent isotopic stationary state reached after 300 s. The labeling rate was consistent with the optimized mixing time of about 4.9 s inside the reactor and the shortest reliable sampling period assessed at 5 s.

Abbreviations: 2/3-PG, 2 and 3-phosphoglycerate; 3PG, 3-phosphoglycerate; 6PG, 6-phosphogluconate; ADP, adenosine diphosphate; AMP, adenosine monophosphate; ATP, adenosine triphosphate; CDP, cytidine diphosphate; Cit, citrate; CLE, carbon labeling experiment; CMP, cytidine monophosphate; CTP, cytidine triphosphate; EMP, Embden-Meyerhof-Parnas; F6P, fructose-6-phosphate; FAME, fatty acid methyl ester; FBP, fructose biphosphate; G1P, glucose-1-phosphate; G6P, glucose-6-phosphate; GDP, guanosine diphosphate; GMP, guanosine monophosphate; GTP, guanosine triphosphate; Gly3P, glycerol-3-phosphate; IDP, inosine diphosphate; IMP, inosine monophosphate; INST, isotopic non-stationary; IsoCit, isocitrate; Man6P, mannose-6-phosphate; MFA, metabolic flux analysis; MID, mass isotopomer distribution; P5P, ribose-5-phosphate, ribulose-5-phosphate and xylulose-5-phosphate; PAR, photosynthetically active radiation; PBR, photobioreactor; PEP, phosphoenolpyruvate; PPP, pentose phosphate pathway; PRPP, phosphoribosyl pyrophosphate; RBP, ribulose bisphosphate; Rib1P, ribose-1-phosphate; RubisCO, ribulose-1,5-bisphosphate carboxylase/oxygenase; TCA, tricarboxylic acid; UMP, uracil monophosphate; UTP, uracil triphosphate.

Correspondence to: G. Cogne

Contract grant sponsor: French National Research Agency project ALGOMICS
Contract grant number: ANR-08-BIOE-002
Contract grant sponsor: FP7 European project
Contract grant number: SOLAR-H2
Contract grant sponsor: Région Midi-Pyrénées
Contract grant sponsor: European Regional Development Fund (ERDF)
Contract grant sponsor: French Ministry for Higher Education & Research
Contract grant sponsor: SICOVAL
Contract grant sponsor: IBiSa
Received 25 March 2012; Revision Revised 30 May 2012; Accepted 31 May 2012
Accepted manuscript online 11 June 2012;
Article first published online 27 June 2012 in Wiley Online Library (http://onlinelibrary.wiley.com/doi/10.1002/bit.24575/abstract)
DOI 10.1002/bit.24575

Introduction

One key factor in bioprocess development and implementation is understanding the role of the biological processes by which the biocatalyst interacts with the imposed environment through the bioreactor system. Among the most recent biotechnological challenges, exploitation of the

photosynthetic capacities of microalgae holds great promise for the production of high-value compounds such as food additives and pharmaceuticals, and for the production of biofuels (Harun et al., 2010; Pruvost, 2011; Spolaore et al., 2006). To develop future strategies to optimize and control the relevant bioprocesses, it is clear that cellular metabolism, as the core of the global reaction process, needs to be thoroughly understood and analyzed. In that context, systems biology approaches are well-suited to gaining an in-depth and comprehensive understanding of the regulatory and metabolic networks of microalgae.

Metabolic flux analysis (MFA) is a powerful tool in systems biology to characterize the behavior of organisms in response to genetic and environmental perturbations. The aim of this experimental and modeling approach is (i) to quantify mass flows through the metabolic network of a microorganism (Wiechert, 2001) and (ii) to analyze flux redistributions in response to changing genetic and (or) environmental conditions (Stephanopoulos, 1998). More specifically, the ^{13}C-MFA method allows the in vivo quantification of metabolic fluxes through metabolic pathways from carbon labeling experiments (CLEs) by combining targeted metabolite analysis with computational modeling (Nöh and Wiechert, 2011; Sokol et al., 2012). It has been successfully applied to many diverse organisms (prokaryotes and eukaryotes) cultivated under ranging physiological conditions (heterotrophy and mixotrophy). To date, ^{13}C-MFA has been little exploited under autotrophic conditions in which CO_2 as a one-carbon unit is the sole carbon source for cell growth (Young et al., 2011). At the start of a CLE, cells cultivated under metabolic steady-state conditions and growing on $^{12}CO_2$ are suddenly fed $^{13}CO_2$ at a set $^{13}C/^{12}C$ ratio. The ^{13}C-labeled substrate is then gradually incorporated into the metabolism via enzyme-catalyzed reactions, until an isotopic steady-state is reached when all the carbon atoms of downstream metabolites are ^{13}C-enriched to the same extent as the feed isotope input. An isotopic steady-state is unable to provide any valuable information to identify flux distributions under autotrophy, and so the transient period of label incorporation must be exploited, requiring short time-scale sampling. This approach is called isotopic non-stationary ^{13}C-MFA (INST ^{13}C-MFA) in the literature (Nöh et al., 2007; Nöh and Wiechert, 2011; Shastri and Morgan, 2007). The experimental design of such investigations requires measuring transient labeling profiles for key metabolites over central and intermediate metabolism, along with their absolute concentrations (assumed to be constant during the labeling experiment) to determine flux distributions through the metabolic network. Only one earlier study in the literature (Young et al., 2011) was performed on a cyanobacteria, *Synechocystis* sp. PCC 6803, under photoautrophic conditions with no discussion about the effect and the controlled dynamics of 13-carbon enrichment of culture medium. Hence the design presented here is an original one, offering highly controlled labeling and culture conditions under photoautotrophy.

The present work focuses on the experimental design of a photobioreactor (PBR) especially conceived for transient isotopic ^{13}C-labeling experiments under photoautotrophic conditions. The experimental set-up provided for (i) a rapid sampling and quenching procedure and (ii) rapid mixing throughout the reactor to ensure a sudden step-change in the ^{13}C-labeled feed from liquid label injection without affecting uptake flux rate. The operating procedure and performance of the experimental device were tested and validated for continuous cultures of the unicellular green alga *Chlamydomonas reinhardtii* grown under metabolic steady-state conditions.

Materials and Methods

Strain and Media

Wild-type *Chlamydomonas reinhardtii* 137AH cells from the culture collection of the French Alternative Energies and Atomic Energy Commission (CEA Cadarache, France) were conserved on solid (agar 1.75%) standard Tris–acetate–phosphate (TAP) medium (Gorman and Levine, 1965) at 16°C and replicated every month. From this, liquid precultures were performed in flasks containing TAP medium and nursed at 25°C under constant stirring at 135 rpm and illumination at approximately 100 μmol m^{-2} s^{-1} in an incubator (New Brunswick Innova® 44). Precultures were replicated every 4 days to keep cells in mid-log phase. After five replications and at a cell density of 4–7×10^6 cells mL^{-1} (corresponding to a late logarithmic growth state), cells were harvested by centrifugation (4,500*g*, 5 min, 20°C in a Sorvall® RC-6 Plus centrifuge) and the cell pellet was resuspended in fresh medium (NH_4Cl 1.45 g L^{-1}, $MgSO_4 \cdot 7\ H_2O$ 0.28 g L^{-1}, $CaCl_2 \cdot 2\ H_2O$ 0.05 g L^{-1}, KH_2PO_4 0.71 g L^{-1}, $NaHCO_3$ 1.68 g L^{-1}, Hutner solution 1 mL L^{-1} (Hutner et al., 1950)). Resuspended cells were then used to inoculate continuous cultures fed with the same fresh medium. Standard culture conditions in photobioreactors were pH 7.5 ± 0.1 and temperature 25 ± 1°C.

Experimental Set-Up

Design and Operation

The experimental set-up was based on a torus-shaped photobioreactor (PBR; Fig. 1) illuminated on one side, already described elsewhere (Fouchard et al., 2008; Pottier et al., 2005; Pruvost et al., 2006). Its working volume was 1.3 L with a specific illuminated area of 25 m^{-1}. The PBR was made of polymethylmethacrylate (PMMA) and was fully transparent except for the rear, which was made of stainless steel. Its front surface was flat and the channel cross-section of the torus was square (gap width 0.04 m), so that light transfer attenuation occurred only along the culture depth, consistent with the approximation of a one-dimensional irradiance profile, which can be characterized by full

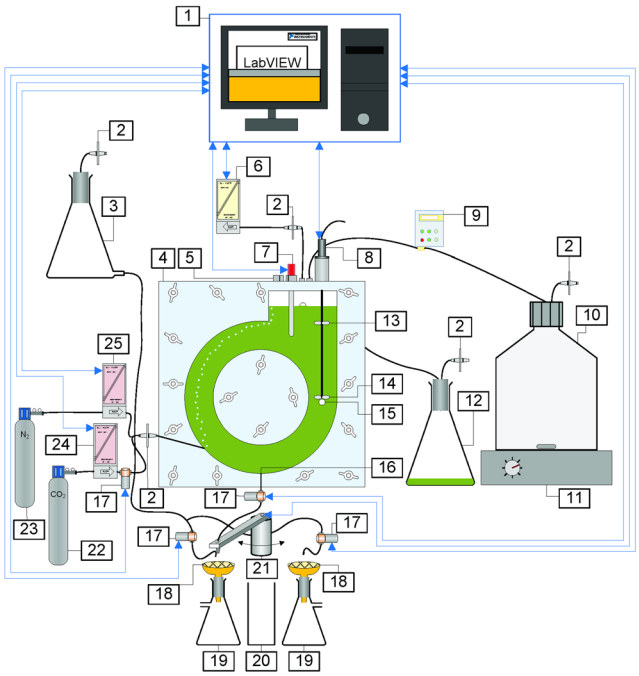

Figure 1. Photobioreactor design for INST ^{13}C-MFA. 1: computer, 2: filter, 3: rinsing solution, 4: torus-shaped photobioreactor, 5: septum, 6: pressure controller, 7: pH and temperature probe, 8: mixing shaft, 9: Stepdos pump, 10: fresh medium, 11: magnetic stirrer, 12: harvest, 13: second impeller, 14: main impeller, 15: injection point, 16: sampling point, 17: valve, 18: fast filtration unit, 19: vacuum flask, 20: waste, 21: stepper motor, 22: CO_2 cylinder, 23: N_2 cylinder, 24: CO_2 mass flow meter, 25: N_2 mass flow meter.

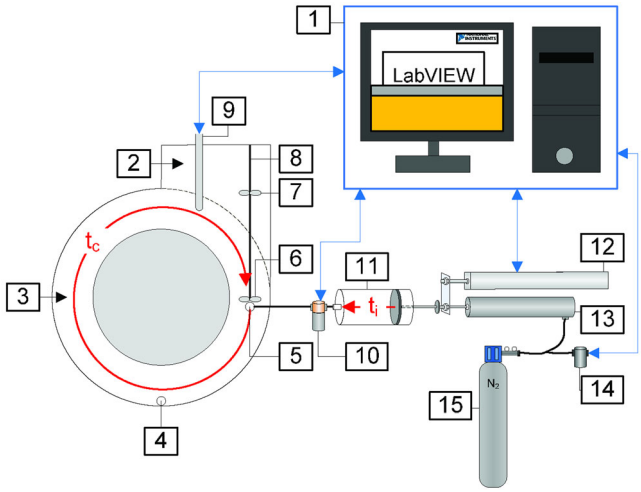

Figure 2. Representation of the experimental mixing strategy using an automated injection device. 1: computer, 2: recirculation zone, 3: plug-flow zone, 4: sampling point, 5: injection point, 6: main impeller, 7: secondary impeller, 8: shaft, 9: conductimetry probe, 10: valve, 11: syringe, 12: rheostat dimmer, 13: pneumatic jack, 14: pressure controller, 15: N_2 cylinder.

modeling of light transfer using a two-flux method (Pottier et al., 2005). The light source was a panel of light-emitting diodes (LEDs), emitting white light within the visible spectrum domain, and the incoming photon flux density (PFD) onto the PBR was controlled. All the experiments were conducted under a constant PFD of 200 μmol m^{-2} s^{-1} (PAR), determined using multi-point measurements with a cosine quantum sensor (LI-190SA, LI-COR®).

In addition to strict control over the radiative transfer process, the torus-shaped PBR provided efficient mixing while keeping shear stress within a reasonable range through its loop configuration (Pruvost et al., 2006). Stirring was enhanced by using two marine impellers attached to the same shaft at different heights (Figs. 1 and 2). Stirring speed could be set from 0 to 4,000 rpm and was calibrated with a stroboscope. The impeller rotation speed during all the experiments was set to 300 rpm, except for the duration of the labeling injection, when it was increased by 900 rpm to accelerate mixing in the PBR. pH and temperature were monitored and controlled during the experiments (Mettler Toledo® Inpro 3253SG/120/Pt100 probe). pH was kept constant at 7.5 by CO_2 injection using an on-off controlled mass flow controller (EL-FLOW F-201CV-020-RAD-33-Z, Bronkhorst®, Montigny-Les-Cormeilles, France) at a constant flow rate of 3 mL min^{-1}, except during CLEs where pH was controlled by adding hydrochloric acid (HCl 0.1 N) to avoid any label dilution.

To prevent any metabolic shift toward photorespiratory pathways during growth cultures, nitrogen (N_2, Air Liquide®, Paris, France, 99% pure) as an inert gas was bubbled through the culture broth at a constant flow rate of 10 mL min^{-1} using a mass flow controller (EL-FLOW F-201C-RAD-33-V, Bronkhorst®) to strip oxygen. During sampling, the incoming N_2 flow rate was 60 mL min^{-1} and the pressure of the flowing gas was regulated by a gas pressure regulator (EL-PRESS P-702C-RAB-00R1-33-E, Bronkhorst®). The pressure was set to 124 mbar, relative to atmospheric pressure, and remained constant throughout the sampling duration. The PBR set-up was operated in continuous mode and fed with fresh medium using a dosing pump (Stepdos® pump 03/RC, KNF Neuberger) at a constant dilution rate of 0.04 h^{-1}. The culture volume was kept constant by harvesting culture using a peristaltic pump (Masterflex® LS Easy-Load II) at the same flow rate. A septum on the top of the PBR allowed daily manual sampling for analysis.

A data processing system (DAQ 6023E-National Instruments®, Austin, TX) was used for automated on-line data acquisition and process control. The software was written with the LabView Virtual Instruments programming techniques (National Instruments®).

Rapid Step-Change in the ^{13}C-Labeled Feed

The ^{12}C/^{13}C switch had to be performed over time following a rapid step-change in order not to affect the observed labeling dynamics of quantifiable metabolites (Shastri and

Morgan, 2007). *Chlamydomonas reinhardtii* uses inorganic carbon as a carbon source and is able to take up and utilize both predominant inorganic carbon species present in culture medium at pH 7.5, that is, CO_2 and HCO_3^- (Spalding, 2008). Considering the slow carbon turnover rates in culture medium under gas–liquid mass transfer (Degrenne et al., 2010), labeled carbon (^{13}C) was injected in a dissolved liquid form. The originality of the experimental framework lay in the control of mixing in a torus-shaped reactor with plug-flow hydrodynamics (Fig. 2). Mixing was obtained by recirculating fluid through the loop with an impeller, ensuring efficient dispersion of the injected labeled solution (Pruvost et al., 2006). Considering the specific hydrodynamics, it is theoretically possible to approach a step-change in the $^{13}C/^{12}C$ ratio of the carbon feed by uniformly injecting the label over a period equal to the circulation time inside the torus-shaped PBR. In this case, the mixing time would be ideally equal to the circulation time, which can be reduced by increasing the impeller rotation speed.

One single injection point located just below the main flow impeller was used (Figs. 1 and 2) for a rapid, efficient dispersion of the injected labeled substrate solution. In order to reach a maximum ^{13}C-labeling enrichment without disturbing the metabolic steady-state of the culture, the injected volume was set at 50 mL (representing 4% of the PBR working volume and corresponding to a dilution factor of 1:26). The injected carbon source was composed of dissolved inorganic carbon in aqueous solution (1 M).

Rapid Sampling and Quenching Methods

Measuring intracellular transient labeling states requires rapid, reliable sampling to assess kinetics of the ^{13}C incorporation into the metabolites (Shastri and Morgan, 2007). Here, a rapid sampling system was developed consisting of an automatic fast filtration method coupled to a manual rapid liquid nitrogen quenching step. Samples were alternately deposited on polyamide filters (Sartorius®, Goettingen, Germany, 25007–47N, 0.2 μm) placed on two sintered glass vacuum filtration units through a rotating arm moved by a step-by-step motor at a controlled fast sampling frequency (Fig. 1). The single sampling point was located at the bottom of the PBR (Fig. 2). The sampling volume was controlled by the sampling time through a valve (SMC VDW21-5G-2-01F-Q) and kept constant by regulating the pressure in the PBR. The sampling volume was set at 512 ± 4 μl with a valve opening time of 90 ms. In order to remove extracellular salts, the filters were quickly and automatically rinsed with 1 mL of rinsing solution (NH_4Cl 1 g L^{-1}, $CaCl_2 \cdot 2\ H_2O$ 0.05 g L^{-1}, KH_2PO_4 0.2 g L^{-1}) after sample filtration. Filters were then manually collected and quenched in liquid nitrogen (−196°C; Bolten et al., 2007). Before each sampling event, the tubing of the sampling system was systematically purged for 800 ms, corresponding to a volume of about 2 mL.

Analytical Protocols

Biomass Dry Weight

Cell dry weight (DW) concentrations C_x were determined by filtering a constant volume V of culture on pre-dried (110°C for 24 h) and pre-weighed (Mettler Toledo, AB204) filters (Whatman®, Kent, UK, GF/F). Cells were rinsed with de-ionized water before drying at 110°C for 24 h. The filter weight difference for the given volume V allows the estimate of biomass concentrations C_x expressed in g DW L^{-1}.

Volume Repeatability

In order to test the volume repeatability of the sampling method, forty-three 500 μl aliquots of de-ionized water were sampled according to the sampling procedure presented above. All the samples were weighed (Mettler Toledo, AB204) before and after sampling to determine their corresponding volumes.

Fatty Acid Methyl Ester (FAME) Analysis

High performance liquid chromatography (HPLC) grade solvents were purchased from VWR International® (Fontenay-sous-Bois cedex, France). Butylated hydroxytoluene (BHT), boron trifluoride (BF_3, 14% by weight in methanol), glyceryl triheptadecanoate (TG17:0) and 37-component fatty acid methyl esters (FAMEs) were obtained from Sigma–Aldrich®. Glassware was systematically heated for 6 h at 450°C to limit organic pollution. Thirteen 500 μl replicates of fresh culture were sampled in glass vials from the PBR. Samples were centrifuged at 3,600*g* (10 min, 4°C) to pellet the cells. Microalgae lipid extraction was conducted by resuspending cells in 6 mL of chloroform/methanol mixture (2:1, v:v). To ensure complete lipid extraction, vials were sonicated eight times at 4°C for 10 s and maintained for 6 h under agitation at room temperature. After adding 0.01% (w/w) of BHT as antioxidant, extracts were stored at −20°C under nitrogen before analysis. Lipid extracts were dried under nitrogen. After adding 1 mL of BF_3 and 10 μg of TG17:0 as internal standard, samples were then transesterified for 10 min at 100°C. After cooling and adding 1 mL of hexane, the organic phase, containing FAMEs, was washed three times with 1.5 mL of water-saturated hexane. FAMEs were recovered and analyzed with a Thermo® Focus gas chromatograph (GC; Waltham, MA) equipped with an on-column injector, a TR-FAME capillary column (Thermo®) and a flame ionization detector. FAMEs were identified by comparing their retention times with known standard mixtures such as 37-component FAMEs. FAME mass composition and quantity in samples were determined from their respective FAME chromatograms obtained by GC, as a proportion of the quantity of TG17:0. Integration and calculation were performed using the software program ChromCard 2.4.1 (Thermo®).

Metabolite Analysis

Differential Method. The differential method (Taymaz-Nikerel et al., 2009) was used to quantify intracellular metabolites under metabolic steady-state conditions. Intracellular metabolite concentrations were obtained by subtracting extracellular from total culture measurements. About 60 intracellular metabolites could be detected. Alongside labeling experiments, five 500 μl replicates of culture or filtered culture (Sartorius®, Minisart NML, 0.45 μm) were taken through the PBR septum and added to 5 mL of boiling 75% (v/v) ethanol and kept at 95°C for 20 s, combining metabolite extraction and quenching in one single step. Extraction was stopped by immersing sample tubes in a −80°C 75% (v/v) ethanol bath. The alcohol phase was then evaporated off by vacuum centrifuge, and the pellet lyophilized and resuspended in 125 μl of de-ionized water before analysis. Uniformly ^{13}C-labeled cell extracts of *C. reinhardtii* grown on [^{13}C]carbon dioxide were used as an internal standard for subsequent metabolite quantification according to the isotope dilution mass spectrometry (IDMS) method described by Wu et al. (2005). The IDMS standard was added simultaneously to both cultures and filtrates during the extraction step. The addition of the IDMS allowed the absolute quantification of 29 metabolites and relative quantification for most other compounds.

Fast Filtration Method. Filters resulting from rapid sampling and quenching methods (see above; Bolten et al., 2007) were immersed in 5 mL of boiling water (99°C) and then extracted for 60 s in a water bath (99°C). Samples were freeze-dried and resuspended in 125 μl of de-ionized water before analysis. As with the differential method, IDMS standard was added to samples collected by fast filtration to carry out metabolite quantification.

Metabolite Analysis and Data Processing. Metabolites were analyzed by ion-exchange chromatography coupled with tandem mass spectrometry (IC-MS/MS) using the method described in Bolten et al. (2007). Samples were analyzed using ion chromatography (Dionex ICS 2500) coupled to a Q-Trap 4000 Triple Quadripole mass spectrometer used in multiple reaction mode. Out of 60 intracellular metabolites that were detected, absolute quantification could be achieved for 29 metabolites using the isotopic dilution mass spectrometry (IDMS) technique (Wu et al., 2005). The ^{13}C-mass isotopomer distributions (MIDs) of 21 intracellular metabolites belonging to central carbon metabolism were determined from relevant isotopic clusters in the IC-MS/MS analysis, according to Kiefer et al. (2007), for each of the 58 samples collected during CLE. The isotopic clusters were corrected for the natural abundance of isotopes other than ^{13}C using the home-made software IsoCor (Millard et al., 2012), available at http://metasys.insa-toulouse.fr/software/isocor/.

Circulation and Mixing Time Measurements

Circulation and mixing times were measured using a conductimetry method. The conductimeter (Tacussel® CD810, Radiometer Analytical S.A., Villeurbanne, France) recorded a signal linearly related to tracer concentration via the conductimetry probe (Radiometer® XE100, Radiometer Analytical S.A., Villeurbanne, France), located on the top of the PBR in place of the pH and temperature probe (Fig. 2). Circulation and mixing times were measured (Fig. 6) after a sudden 10 mL pulse of sodium chloride tracer (NaCl 1.7 M). Mixing times were subsequently estimated from an automated linear time-varying injection of NaCl (1 M) using a 50 mL plastic piston syringe (representing 4% of the PBR working volume) driven by a pneumatic jack (Fig. 2). A rheostat dimmer, fixed parallel to the pneumatic jack, measured the rate and uniformity of the syringe piston movement normalized by the piston stroke length as injection progressed (Fig. 6), from which injection time could be deduced. An overpressure inside the reactor was maintained by N_2 gas flow throughout the measurements of circulation and mixing times to recreate carbon labeling experiment conditions.

Carbon Enrichment Measurements

The protocol consisted in measuring total dissolved inorganic carbon concentration during a carbon labeling test experiment. Three measurements were performed before injection, after injection and inside the injected solution. The carbon enrichment was defined as the ratio between pulsed and total inorganic carbon measurements after injection. Total dissolved inorganic carbon concentrations were measured using a total carbon analyzer (TOC 5000 Shimadzu®, Marne-la-Vallée Cedex 2, France).

Results and Discussion

Critical Analysis of the Sampling System

Sampling Homogeneity and Performance

The rapid inactivation of cellular metabolism is necessary to observe a real metabolic state representative of the imposed culture conditions with no artifact from a steady-state break (Nöh and Wiechert, 2011). Owing to the rapid turnover of metabolites involved in many metabolic reactions, sampling has to be done in seconds. In our case, a sampling time lapse of at most 5 s was obtained from culture broth up to quenching (metabolism freeze) in liquid nitrogen. Because of the design choice described above, which provided for sampling at one single point at the bottom of the PBR, it was not possible to replicate samples. However, the sampling device could operate at a relatively high frequency. Using this device, over 60 intracellular metabolites could be detected in cellular extracts by IC-MS/MS, and absolute quantification could be achieved for 29 metabolites using the IDMS technique (Wu et al., 2005). The analysis of metabolite pools in samples collected for different sampling periods (10 samples per period) showed that stable

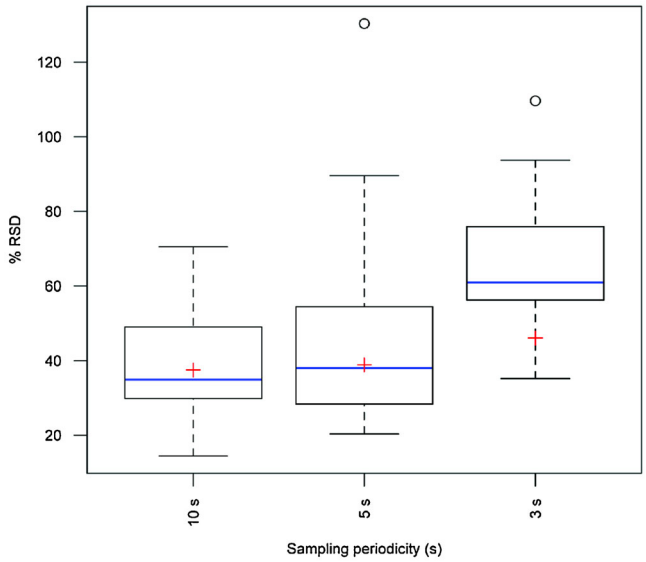

Figure 3. Metabolic repeatability assays as a function of sampling period. Mean relative standard deviations (% RSD) were measured for 10, 5, and 3 s sampling periods. Box plots include medians (blue lines) and means (red crosses).

metabolome contents could be obtained with 5 and 10 s sampling periods, but not 3 s, which clearly stood out from the other times in terms of standard deviations (Fig. 3). Hence, further sampling was performed using periods of 5 s or more. It was also observed that a limit sampling period of 5 s had to be applied so as not to disturb the PBR overpressure, which affected sampling volume and so downstream analysis, as observed using a 3 s period. To control the quality and quantity of the sampled biomass, the sampling system repeatability was assessed by measuring sampling volumes and total fatty acid methyl ester (FAME) contents, used as indicators of biomass concentrations (Table I). Volumes and total FAME measurements were found to be highly repeatable, with mean relative standard deviations of 0.75% and 3.88%, respectively, which may be mainly due to measurement uncertainties. This rigorous sampling process provided metabolite quantifications with a mean relative standard deviation of 24.80% (Table I), which is in the usual order of magnitude of metabolomic standard deviations. We also note that all these results indicate no difference between right and left filtration units, which presented similar mean standard errors. Some metabolites showed high relative standard deviations, due either to small signal-to-noise ratios in MS/MS spectra or to contaminations, classically observed for organic acids when highly sensitive LC/MS methods are employed.

In Situ Validation

A non-stationary carbon labeling experiment was carried out by injecting a saturated $NaH^{13}CO_3$ solution (84 g L^{-1}) into a continuous culture under metabolic steady-state.

Table I. Sampling homogeneity and repeatability.*

Measure	Value	SD	%RSD
Volume (µL)	512.02	3.82	0.75
Fatty acid methyl esters (mg g^{-1} DW)			
16:00	18.29	0.35	1.90
16:1n-9	1.88	0.06	2.98
16:1n-7	2.65	0.10	3.72
16:2n-6	0.90	0.04	4.64
16:2n-4	1.21	0.05	4.20
16:3n-3	1.79	0.09	4.88
16:4n-3	13.11	0.69	5.26
18:00	2.33	0.04	1.82
18:1n-9	6.87	0.22	3.16
18:1n-7	2.85	0.09	2.97
18:2n-6	7.11	0.33	4.65
18:2n-4	6.10	0.28	4.60
18:3n-3	18.78	0.92	4.92
Non-identified	1.69	0.08	4.54
Mean			3.88
Metabolites (µmol g^{-1} DW)			
2/3-PG	8.82	0.80	9.06
6PG	0.22	0.04	20.00
ADP	4.22	0.16	3.76
AMP	1.93	0.15	7.99
ATP	6.08	0.45	7.45
CDP	0.25	0.03	13.52
Cis-Aconitate	0.01	0.01	76.31
Cit	0.20	0.24	123.33
CMP	0.10	0.02	21.37
CTP	0.83	0.24	28.82
F6P	0.91	0.07	7.70
Fumarate	0.60	0.24	40.15
G6P	2.70	0.33	12.29
GDP	0.70	0.21	29.87
GMP	0.18	0.05	30.58
IDP	4.40	0.59	13.32
IMP	0.03	0.01	25.90
IsoCit	0.03	0.02	53.88
Malate	3.27	0.99	30.25
Man6P	0.42	0.07	17.26
P5P	0.95	0.24	24.89
PEP	1.79	0.05	2.79
PRPP	0.08	<0.01	5.42
RBP	0.18	0.04	23.10
Rib1P	0.02	0.01	33.02
UDP	1.17	0.05	4.29
UMP	3.02	0.36	11.86
UTP	1.41	0.23	16.34
Mean			24.80

Absolute value, standard deviation (SD), and relative standard deviation (% RSD in percentage) of sampling volume ($n = 43$), fatty acid methyl ester composition ($n = 13$) and absolute metabolite concentrations ($n = 5$) are presented as repeatability assays measured at metabolic steady-state.

*Probably one single unsaturated C18 FAME.

Fifty-eight samples were collected by fast filtration for 7 min to monitor the kinetics of ^{13}C-label incorporation. Transient isotopic measurements were performed by IC-MS/MS, and isotopic labeling profiles of 21 central metabolites belonging to the Calvin–Benson cycle, pentose phosphate pathway (PPP), Embden–Meyerhof–Parnas (EMP) pathway, tricarboxylic acid (TCA) cycle and phosphonucleotide pathway were specifically investigated. Transient isotopomer fractions of central metabolites after injection showed rapid

incorporation of ^{13}C in central metabolites resulting in a fast decrease in the unlabeled pool and replacement by labeled molecules until the isotopic steady-state was reached (Fig. 4). At this final stage, mass isotopomer distributions (MIDs) remained stable and were directly dependent on the ^{13}C enrichment of the carbon source. The kinetics of ^{13}C-label incorporation in metabolites (Fig. 5) showed that a 5 s sampling interval was appropriate for precise monitoring of label propagation in metabolites. This sampling interval was particularly suitable for providing information on the very first labeling events occurring just after the injection of the label. To further analyze the labeling kinetics in the various metabolites, the ^{13}C cellular enrichment (fraction of ^{13}C atoms incorporated in a metabolite) was calculated. Taking all the analyzed metabolites, the results showed marked differences in ^{13}C-incorporation rates: most of them did not reach the isotopic steady-state by the end of the sampling period (Fig. 5). 2- and 3-phosphoglycerate (2/3-PG, analytically detected as a single metabolic pool) followed by phosphoenolpyruvate (PEP) presented the fastest labeling rates, reaching isotopic steady-state approximately 300 s after injection. These results were fully consistent with basic knowledge of photoautotrophic carbon assimilation by the Calvin cycle through which a carbon unit is captured by ribulose bisphosphate (RBP) and then cleaved into two 3-phosphoglycerate (3PG) molecules

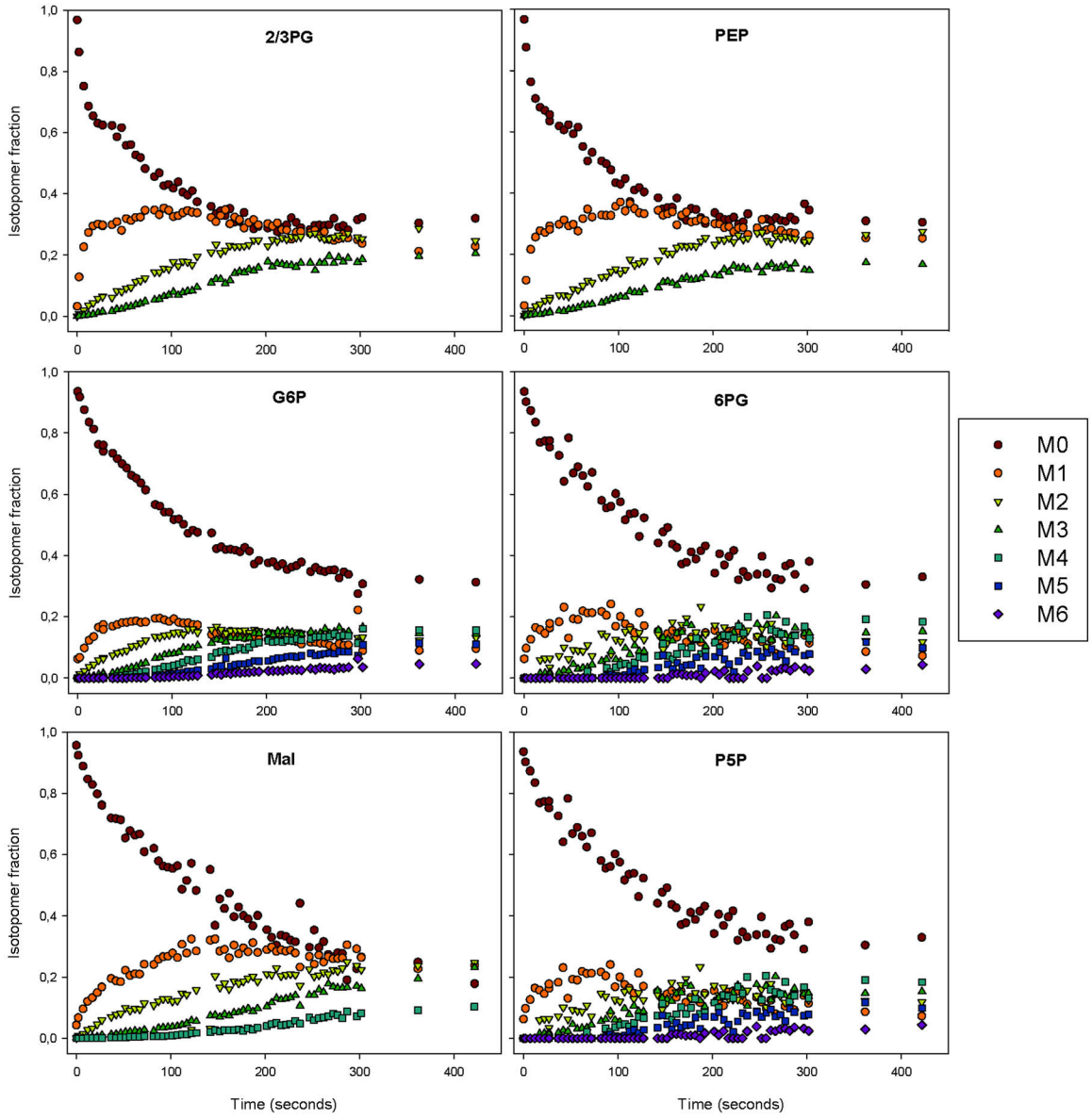

Figure 4. Transient isotopomer fractions of 9 of the 21 central and intermediate metabolites. 2/3-PG: combined pools of 2- and 3-phosphoglycerate, 6PG: 6-phosphogluconate, G6P: glucose-6-phosphate, Mal: malate, P5P: ribose-5-phosphate, ribulose-5-phosphate and xylulose-5-phosphate, PEP: phosphoenolpyruvate.

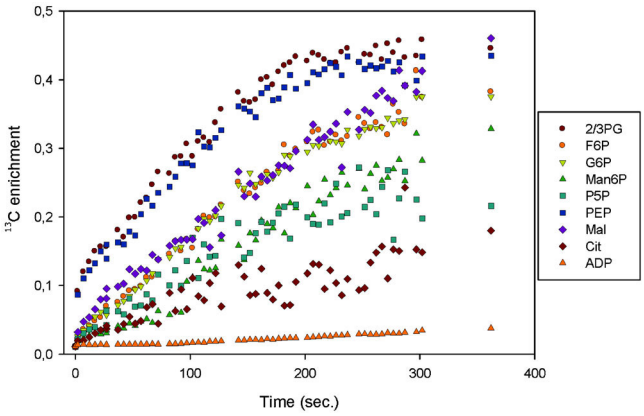

Figure 5. Metabolite ^{13}C enrichment. ^{13}C enrichment of 9 metabolites was calculated using the formula $(1/N)\sum_{i=1}^{N} M_i \times i$, where N is the number of carbon atoms in the metabolite and M_i the fractional abundance of the ith mass isotopomer. 2/3-PG: combined pools of 2- and 3-phosphoglycerate, 6PG: 6-phosphogluconate, ADP: adenosine triphosphate, Cit: citrate, F6P: fructose-6-phosphate, G6P: glucose-6-phosphate, Mal: malate, Man6P: mannose-6-phosphate, P5P: ribose-5-phosphate, ribulose-5-phosphate and xylulose-5-phosphate, PEP: phosphoenolpyruvate.

by RubisCO inside the chloroplast. 3PG can be recycled in a Calvin cycle or exported from chloroplast to cytosol to enter the EMP pathway. We note that the latter pathway seemed to be operative considering the rapid ^{13}C enrichment of PEP.

Label Injection

Mixing Control

PBR Geometry and Experimental Strategy. The ^{13}C-labeling experiment required a rapid step-change in the ^{13}C proportion in the substrate feed in order to measure only the dynamics of label incorporation into cells and not overall dynamics, which would include the ^{13}C-enrichment in the feed with a relaxation time of the same order of magnitude as the metabolic responses. Here the experimental strategy was to incorporate the labeled carbon into the cultivation system by liquid injection, while controlling the mixing process to minimize mixing time. To this end, a typical control procedure was designed, consisting in uniformly injecting label over a time period close to the circulation time in a torus plug-flow reactor. We note that the behavior of the reactor was not completely ideal. Two distinct areas inside the PBR could be observed from coloring agent injection: the circular shape presenting dispersed plug-flow hydrodynamics with recirculation (Benkhelifa et al., 2000) and a dead zone where the sensors were located (Fig. 2). These two areas overlapped, making it difficult to delineate them and predict hydrodynamics and mixing for this PBR geometry. To minimize the effect of this dead zone on mixing, a second impeller was added on the shaft and the influence of impeller height on the circulation time was measured (data not shown). An optimal height was determined to obtain the shortest circulation time. Because of the PBR loop geometry, circulation time could also be shortened by increasing stirring speed from 300 rpm (routine speed) to 900 rpm (only during label injection) while keeping shear stress within a reasonable range (Pruvost et al., 2006).

Circulation Time Measurements. The circulation time is defined as the time interval between successive passes of a liquid through the same or a corresponding point in a stirred vessel. In the particular case of a torus-shaped reactor with plug-flow hydrodynamics, it can be more simply defined as the time needed to make one loop inside the torus. Practically, circulation time is the mean time lapse between two consecutive oscillatory peaks obtained from conductivity monitoring after a spot tracer injection. By increasing stirring speed from 300 to 900 rpm, circulation time was found to decrease significantly from 6 to 7 s to 2.04 ± 0.03 s (Fig. 6). This mean value presents a standard deviation of 1.5%, strengthening the reliability of the measure.

Mixing Time Characterization. Mixing time is the time required from injection (t_0) to achieve a certain degree of homogeneity defined here by the final tracer concentration within 5%. For instance, a mixing time of 15.87 s is observed after a spot tracer injection (Fig. 6). To shorten mixing time as explained above, the injections were performed using an automated injection device. The repeatability and reliability of this device, in terms of injected volume and uniformity of syringe piston movement, were tested. Ten syringe volume measurements gave 50.14 ± 0.08 mL, which corresponds to a relative standard deviation of 0.16%. We note that the injection progress curves show identical and perfectly uniform linear movements during injection (with coefficients of determination R^2 of 0.999; Fig. 7). These results confirm the excellent repeatability of the automated injection procedure. Injection time was fitted on a previously measured circulation time of 2.04 s. Four similar injections were performed for a mean injection time of 2.10 ± 0.02 s. A mean mixing time of 4.88 ± 0.08 s was determined (Fig. 7). As depicted, the four independent replicates overlay each other, showing a good repeatability of the mixing inside the PBR.

pH Control and Carbon Enrichment

The injection of bicarbonates causes a pH change, due to their pK_a of 10.3. To prevent this change, buffer can be added to the culture media or to the injected solution. As classic buffers such as Tris, HEPES, MOPES, or PIPES are incompatible with IC analysis, phosphate buffer was used at a concentration of 10 mM. The culture medium was thus reformulated as follows: $NH_4Cl{\cdot}0.725\ g\ L^{-1}$, $MgSO_4{\cdot}7H_2O$ $0.14\ g\ L^{-1}$, $CaCl_2{\cdot}2H_2O$ $0.05\ g\ L^{-1}$, $KH_2PO_4{\cdot}0.305\ g\ L^{-1}$, $NaHCO_3{\cdot}0.84\ g\ L^{-1}$, Hutner solution $1\ mL\ L^{-1}$. Concerning the injected solution, no major change was made, except for $NaHCO_3$ (0.7 M) with pH regulated at 7.5 by bubbling

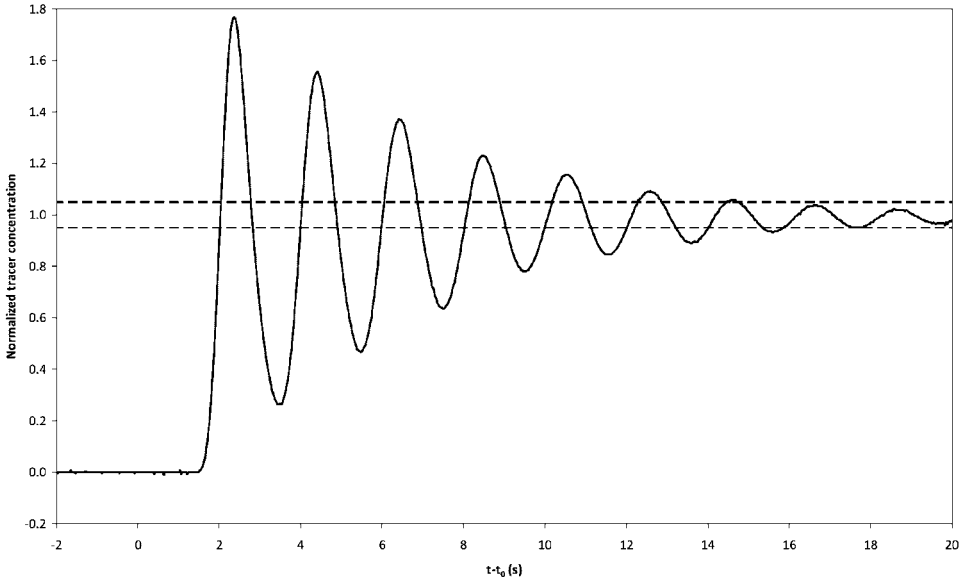

Figure 6. Mixing inside the torus-shaped photobioreactor after a pulse of tracer. After a rapid labeling injection (t_0), tracer concentration (line) oscillates until it reaches its final concentration within 5% (area between the two dashed lines).

the bicarbonate conjugate acid, that is, CO_2. These medium optimizations enabled us to considerably reduce the pH step to 0.06. We note that pH tended to increase due to cell growth and stripping of dissolved carbon dioxide from the culture broth by the nitrogen supply. To restrict this increase, nitrogen gas was flushed directly through the headspace of the PBR. Also, pH regulation by CO_2 injection usually compensates for pH increase, but also enriches the culture medium with dissolved inorganic carbon. Accordingly, CO_2 injection was stopped during CLE so as

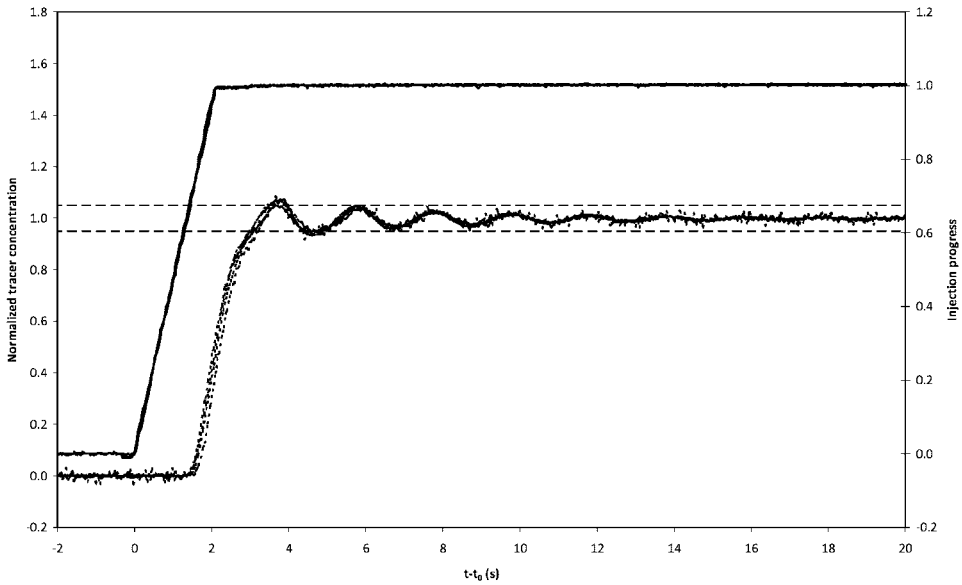

Figure 7. Mixing inside the torus-shaped photobioreactor after a controlled step injection of tracer. Injection progress (lines) allows measurement of injection time while controlling the uniformity of syringe piston movements. Labeling concentrations (dotted lines) reach final concentration within 5% (area between the two dashed lines). Four overlaying assays are presented.

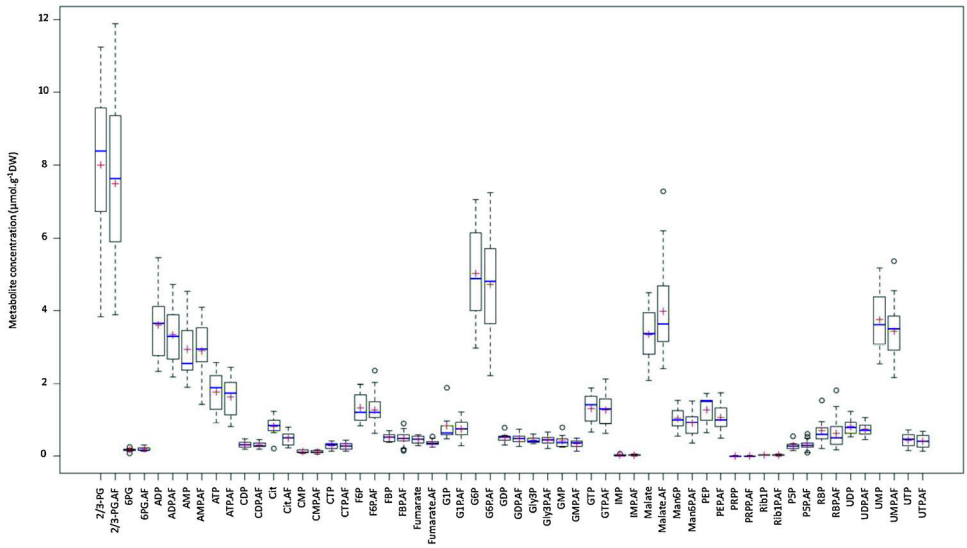

Figure 8. Mean metabolite concentrations during CLE. For each of the 29 metabolites measured, concentrations are compared two by two, before and after injection (AF). Box plots include medians (blue lines) and means (red crosses). Thirty-six samples were collected from 10 min before (seven samples) until 20 min after (29 samples) injection to recreate CLE conditions.

not to modify controlled carbon enrichment, and pH was regulated by addition of acid.

The test CLE was performed in the absence of cells, using ^{12}C instead of ^{13}C for culture medium preparation, in order to assess carbon enrichment. From an inorganic carbon concentration of 10.7 mM, injection led to final concentration of 38.8 mM (i.e., about 2.6-fold enrichment). We note that measured inorganic carbon concentration inside the syringe (0.85 M) before injection would theoretically have led to a final concentration inside the PBR of 43.0 mM. Despite the loss, most probably due to carbon desorption from the injected solution under the sudden pressure release during injection, the measured enrichment (i.e., 72%) was sufficient for us to expect good quality transient isotopomer profiles insofar as it would not disturb the metabolic steady-state. We note that the enrichment might be improved by decreasing the concentration of total inorganic carbon in the culture medium before injection.

Impact of Carbon Enrichment on Metabolic Steady-State

The carbon labeling experiment presented relies on dissolved ^{13}C introduction inside the PBR, which implies at the same time an increase in total dissolved carbon concentration and a change in the $^{13}C/^{12}C$ ratio. To ensure that the observed mass isotopomer profiles were due only to the change in the $^{13}C/^{12}C$ ratio and not to the carbon enrichment, steady-state was checked in the carbon labeling experiment. A test CLE using unlabeled bicarbonate was carried out. The relative concentrations of 29 metabolites were measured on 36 samples from 10 min before until 20 min after injection. No significant differences were observed before and after injection for any metabolites in terms of mean absolute concentrations or statistical distributions (Fig. 8). This demonstrates that the metabolic steady-state was not disturbed by the increase in inorganic carbon concentration in the medium and validates the whole experimental procedure to perform INST ^{13}C-MFA under autotrophy.

Conclusion

Besides allowing culture under highly controlled conditions, the experimental photobioreactor presented features original improvements especially designed for INST ^{13}C-MFA under autotrophic conditions. The sampling procedure presented enables fast, repeatable and reliable sampling that meets non-stationary experiment requirements. The controlled labeling injection system coupled to the mixing strategy developed allows a minimal mixing time of about 5 s, short enough to ensure measurement of real transient isotopic incorporation into metabolites with no delay due to progressive ^{13}C enrichment. It was also shown that the steep increase in carbon concentration due to label injection does not disturb the metabolic steady-state inside the PBR. All the results presented validate the experimental design as appropriate to perform INST ^{13}C-MFA under autotrophic conditions.

The authors thank Hélène Marec and Didier Le Goff for their technical assistance. Part of this work was carried out at MetaToul (Metabolomics & Fluxomics Facilities, Toulouse, France).

References

Benkhelifa H, Legrand J, Legentilhomme P, Montillet A. 2000. Study of the hydrodynamic behaviour of the batch and continuous torus reactor in laminar and turbulent flow regimes by means of tracer methods. Chem Eng Sci 55(10):1871–1882.

Bolten CJ, Kiefer P, Letisse F, Portais JC, Wittmann C. 2007. Sampling for metabolome analysis of microorganisms. Anal Chem 79(10):3843–3849.

Degrenne B, Pruvost J, Christophe G, Cornet JF, Cogne G, Legrand J. 2010. Investigation of combined effects of acetate and photobioreactor illuminated fraction in the induction of anoxia for hydrogen production by *Chlamydomonas reinhardtii*. Int J Hydrogen Energy 35(19): 10741–10749.

Fouchard S, Pruvost J, Degrenne B, Legrand J. 2008. Investigation of H_2 production using the green microalga *Chlamydomonas reinhardtii* in a fully controlled photobioreactor fitted with on-line gas analysis. Int J Hydrogen Energy 33(13):3302–3310.

Gorman DS, Levine RP. 1965. Cytochrome f and plastocyanin: their sequence in the photosynthetic electron transport chain of Chlamydomonas reinhardi. Proc Natl Acad Sci USA 54(6):1665–1669.

Harun R, Singh M, Forde GM, Danquah MK. 2010. Bioprocess engineering of microalgae to produce a variety of consumer products. Renew Sustain Energy Rev 14(3):1037–1047.

Hutner SH, Provasoli L, Schatz A, Haskins CP. 1950. Some approaches to the study of the role of metals in the metabolism of microorganisms. Proc Am Philos Soc 94(2):152–170.

Kiefer P, Nicolas C, Letisse F, Portais JC. 2007. Determination of carbon labeling distribution of intracellular metabolites from single fragment ions by ion chromatography tandem mass spectrometry. Anal Biochem 360(2):182–188.

Millard P, Letisse F, Sokol S, Portais JC. 2012. IsoCor: Correcting MS data in isotope labeling experiments. Bioinformatics 28(9):1294–1296.

Nöh K, Wiechert W. 2011. The benefits of being transient: Isotope-based metabolic flux analysis at the short time scale. Appl Microbiol Biotechnol 91(5):1247–1265.

Nöh K, Gronke K, Luo B, Takors R, Oldiges M, Wiechert W. 2007. Metabolic flux analysis at ultra short time scale: Isotopically non-stationary ^{13}C labeling experiments. J Biotechnol 129(2):249–267.

Pottier L, Pruvost J, Deremetz J, Cornet JF, Legrand J, Dussap CG. 2005. A fully predictive model for one-dimensional light attenuation by *Chlamydomonas reinhardtii* in a torus photobioreactor. Biotechnol Bioeng 91(5):569–582.

Pruvost J. 2011. Cultivation of algae in photobioreactors for biodiesel production. Biofuels. Amsterdam: Academic Press. p 439–464.

Pruvost J, Pottier L, Legrand J. 2006. Numerical investigation of hydrodynamic and mixing conditions in a torus photobioreactor. Chem Eng Sci 61:4476–4489.

Shastri AA, Morgan JA. 2007. A transient isotopic labeling methodology for ^{13}C metabolic flux analysis of photoautotrophic microorganisms. Phytochemistry 68(16–18):2302–2312.

Sokol S, Millard P, Portais JC. 2012. influx_s: Increasing numerical stability and precision for metabolic flux analysis in isotope labelling experiments. Bioinformatics 28(5):687–693.

Spalding MH. 2008. Microalgal carbon-dioxide-concentrating mechanisms: Chlamydomonas inorganic carbon transporters. J Exp Bot 59(7):1463–1473.

Spolaore P, Joannis-Cassan C, Duran E, Isambert A. 2006. Commercial applications of microalgae. J Biosci Bioeng 101(2):87–96.

Stephanopoulos G. 1998. Metabolic engineering. Biotechnol Bioeng 58(2–3):119–120.

Taymaz-Nikerel H, de Mey M, Ras C, ten Pierick A, Seifar RM, van Dam JC, Heijnen JJ, van Gulik WM. 2009. Development and application of a differential method for reliable metabolome analysis in *Escherichia coli*. Anal Biochem 386(1):9–19.

Wiechert W. 2001. ^{13}C metabolic flux analysis. Metab Eng 3(3):195–206.

Wu L, Mashego MR, van Dam JC, Proell AM, Vinke JL, Ras C, van Winden WA, van Gulik WM, Heijnen JJ. 2005. Quantitative analysis of the microbial metabolome by isotope dilution mass spectrometry using uniformly ^{13}C-labeled cell extracts as internal standards. Anal Biochem 336(2):164–171.

Young JD, Shastri AA, Stephanopoulos G, Morgan JA. 2011. Mapping photoautotrophic metabolism with isotopically nonstationary ^{13}C flux analysis. Metab Eng 13(6):656–665.